SUPPLEMENTARY MATERIAL

Probing the Determinants of Diacylglycerol Binding Affinity in C1B domain of Protein Kinase Cα

Mikaela D. Stewart*, Brittany Morgan[#], Francesca Massi[#†], and Tatyana I. Igumenova*[†]

*Department of Biochemistry and Biophysics, Texas A&M University, 300 Olsen Boulevard, College Station, TX 77843.

[#]Department of Biochemistry and Molecular Pharmacology, 364 Plantation Street, University of Massachusetts Medical School, Worcester, MA 01605.

[†]Corresponding authors.

E-mail: tigumenova@tamu.edu; Phone: (979) 845 6312; Fax: (979) 845 4946.

E-mail: Francesca.Massi@umassmed.edu; Phone: (508) 856 4501; Fax: (508) 856 6464.

Overexpression and Purification of C1Bα

The expression of SUMO-C1Bα fusion proteins was induced with 0.5 mM IPTG (isopropyl β-D-1-thiogalactopyranoside, purchased from Fisher Scientific) overnight at 15 °C. For natural abundance protein preparations, the cells were induced upon reaching OD_{600} of 0.6-0.8. Isotope labeling of C1Bα was accomplished using the method of Marley et al.[1] The method involved re-suspending cells grown on Luria-Bertani broth in M9 minimal medium, supplemented with 3 g/L of [^{13}C-6]-D-glucose and 1 g/L of $^{15}NH_4Cl$ (Cambridge Isotopes), and inducing over-expression at OD_{600} of 1.8-2.0. Fractionally deuterated protein samples were produced using M9 minimal media containing 75% $^{2}H_2O$, 3 g/L of [^{13}C-6]-D-glucose, and 1 g/L of $^{15}NH_4Cl$. The cells were harvested by centrifugation at 4 °C and lysed at room temperature using a B-PER protein-extraction reagent (Thermo Scientific). The fusion protein was purified using a HisTrap™ HP Ni affinity column (GE Healthcare Life Sciences). The fractions containing fusion protein were pooled and desalted on HiPrep 26/10 desalting column (GE Healthcare Life Sciences) into a buffer containing 20 mM Tris and 150 mM NaCl at pH 7.0. SUMO was cleaved from C1Bα with histidine-tagged SUMO protease at 30 °C in the presence of 1 mM 1,4-Dithiothreitol (DTT). The products of SUMO protease cleavage reaction were loaded onto the HisTrap™ HP Ni affinity column, and the C1Bα was collected in the flow-through fractions. The final purification step was a gel-filtration on a HiPrep 16/60 Sephacryl S-100 column (GE Healthcare Life Sciences) carried out in 50 mM 2-(N-morpholino)ethanesulfonic acid (MES) buffer and 150 mM KCl at pH 6.5.

1. Marley, J., Lu, M. & Bracken, C., A method for efficient isotopic labeling of recombinant proteins, *J. Biomol. NMR* **20** (2001), pp. 71-75.

Figure S1. Chemical shift perturbation analysis of DOG binding to wt and Y123W C1Bα. The chemical shift differences for the ^{15}N and ^{1}H nuclei of the protein backbone were calculated from the spectra shown in Figure 1. β12 and β34 loop regions are shaded. The largest chemical shift changes are observed in the loops and their hinges, indicating that DOG binding affects the conformation of the loops.

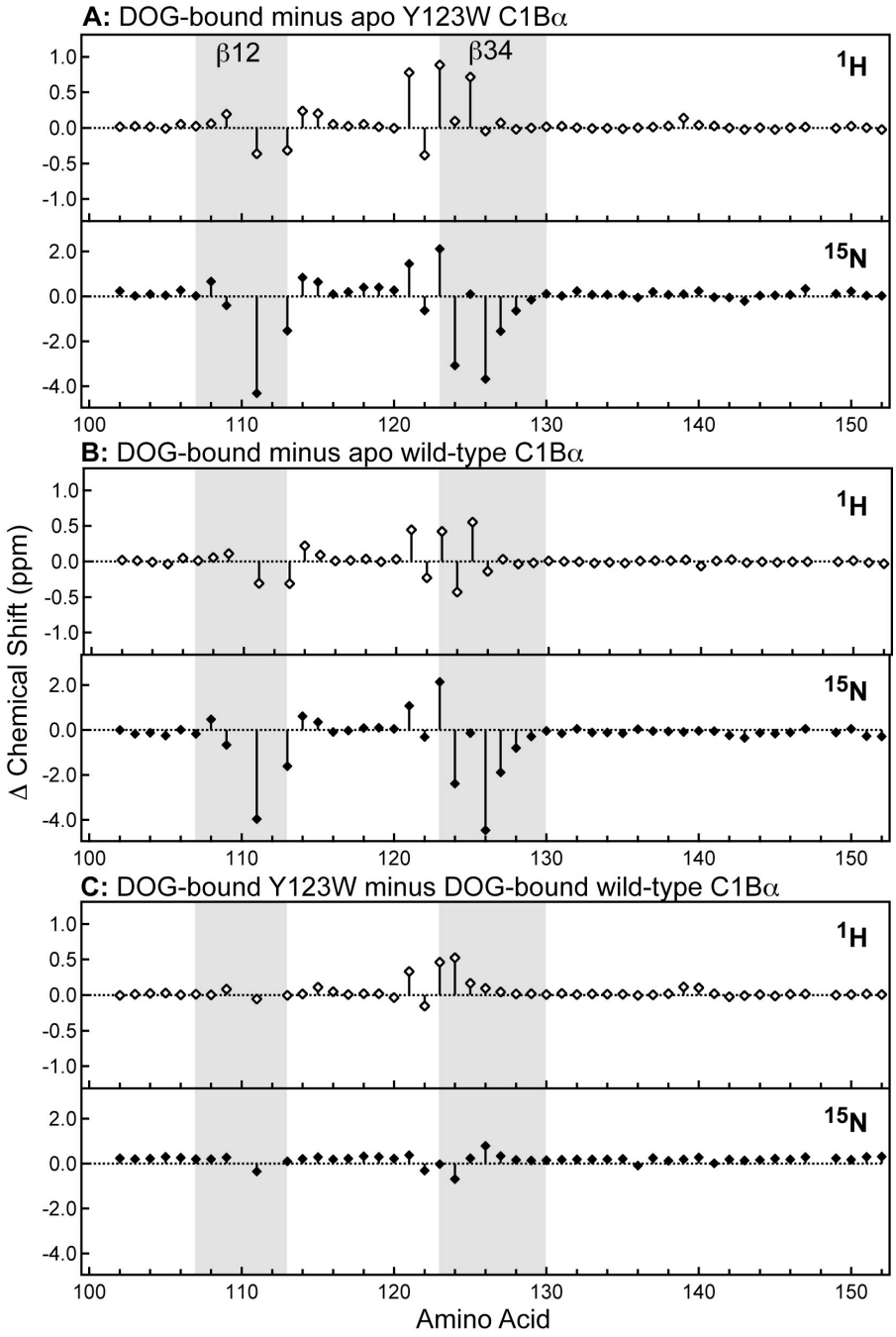

Figure S2. Comparison of the ^{15}N-^{1}H HSQC spectra of the apo-forms of wt and Y123W C1Bα. The cross-peaks for the wt and mutant protein overlap almost exactly, with the exception of the mutation site. The data indicate that the mutation introduces a very minor structural perturbation, as is expected for a solvent-exposed residue such as Tyr123. Asn and Gln side-chain resonances are labeled with asterisks. Residues that show quantifiable dispersion in rotating-frame relaxation dispersion experiments are labeled according to the following scheme: dynamic in both wt and Y123W C1Bα (italicized/bold, blue); wt only (italicized); and Y123W C1Bα (italicized/bold). Residues for which we observed minor chemical shift changes are labeled with a regular font.

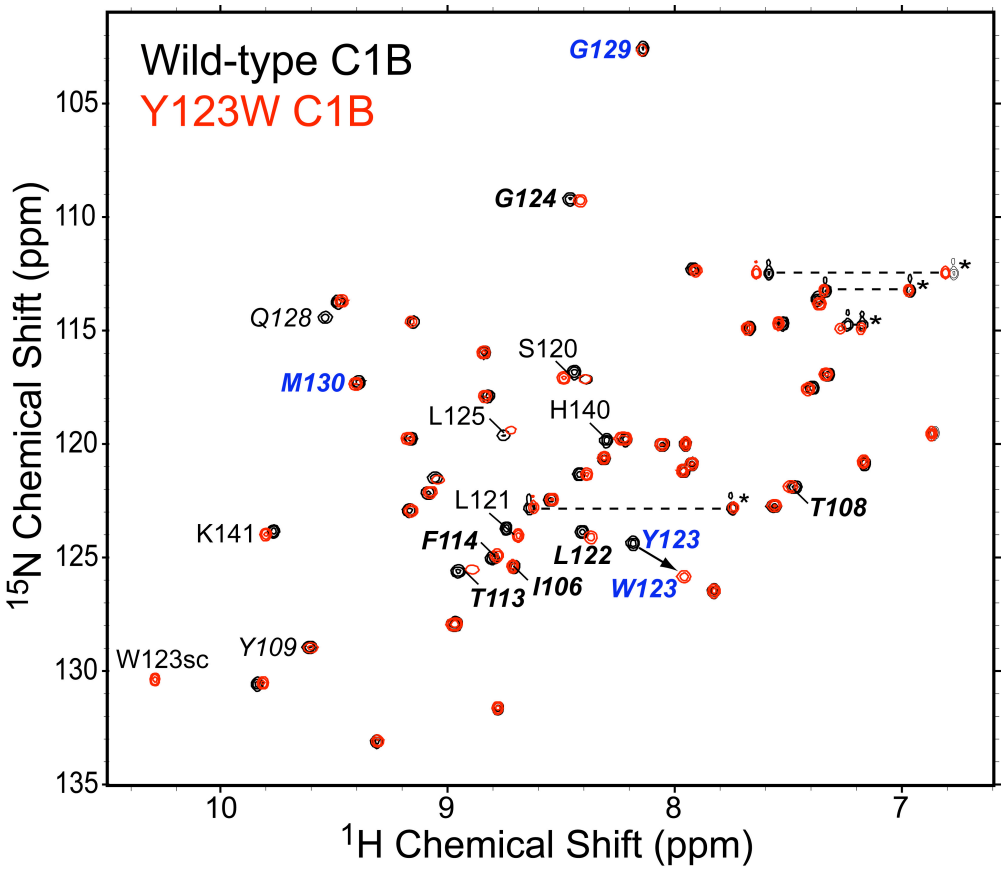

Figure S3. NMR-detected titration of the wt and Y123W C1Bα with phorbol 12,13-dibutyrate (PDBu) in the presence of 10 mM DPC/DPS micelles. The binding process is slow-to-intermediate on the chemical-shift timescale for both wt and Y123W C1Bα indicating comparable PDBu affinities. Large chemical shift perturbations are observed in the apo- versus ligand-bound spectra, suggesting that binding of PDBu to C1Bα with concomitant micelle insertion is accompanied by changes in the conformation of the ligand-binding loops.

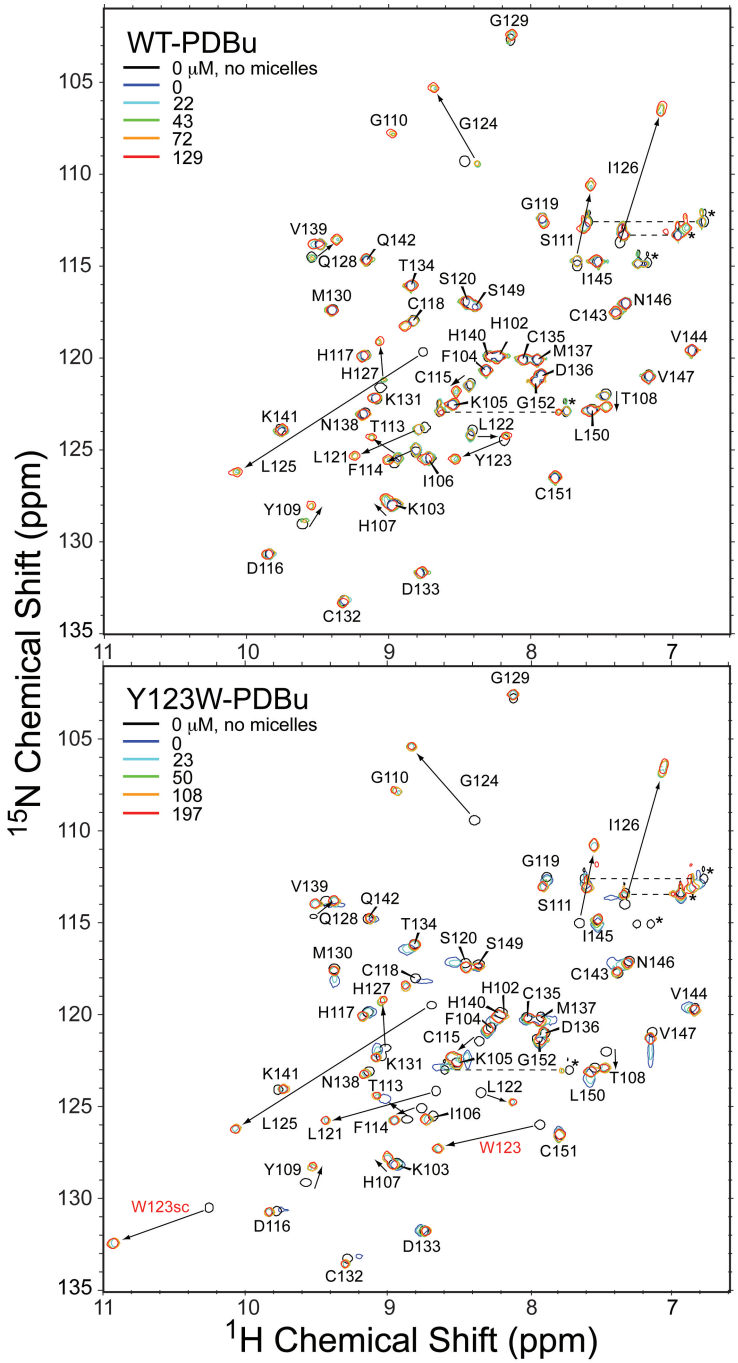

Figure S4. A plot of R_{ex} values obtained in the model-free analysis of wt and Y123W C1Bα. Eight residues the in wt (Tyr109, Tyr123, Gly124, Leu125, Gln128, Gly129, Met130, and Ser149) and thirteen residues in Y123W C1Bα (Thr108, Tyr109, Thr113, Phe114, Leu122, Gly124, Leu125, His127, Gln128, Gly129, Met130, Val147, and Ser149) were fit with Models 3 and 4, which explicitly account for the contribution of chemical exchange to the observed relaxation rates. The differences in the conformational dynamics are pronounced for the hinges of ligand-binding loops β12 and β34.

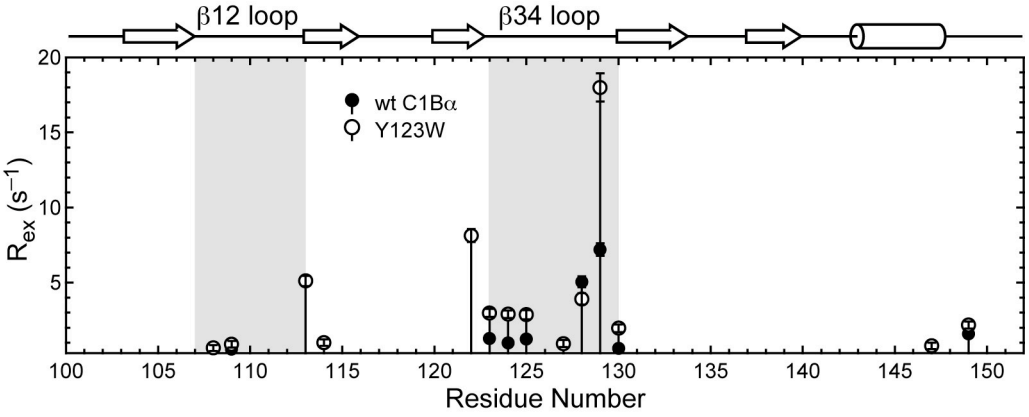

Figure S5. A plot of Φ_{ex} values in Y123W versus wt C1Bα for three residues that show quantifiable dispersion in both proteins. The slope of the fitted line is 1.73 ± 0.03. The population of the excited state is small (< 10-15 %), based on the similarities of population-averaged chemical shifts between the wt and Y123W C1Bα. We can then neglect the term that scales as p_B^2 and re-write the expression for Φ_{ex} (see Eq. (7)) as $\Phi_{ex} \approx p_B \Delta\omega_N^2$. Assuming that $\Delta\omega_N$ values for the wt and Y123W C1Bα are similar for these three residues, the slope of 1.73 would represent the 1.73-fold change in the population of the excited state that occurs as a result of the Y123W mutation.

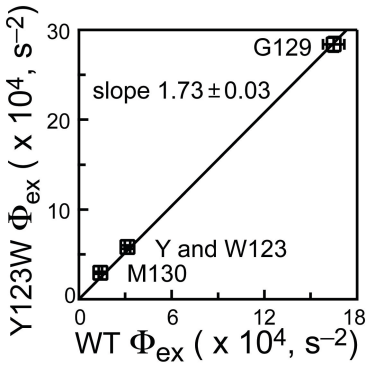

Figure S6. Correlation between the loop tip distance, β12 loop dihedral angles, and hydrogen bonds in Y123W C1Bα. Tip distance (A), dihedral angles of the β12 loop (B), and hydrogen bonds (C) are plotted as a function of time in a representative Y123W C1Bα trajectory. The closed-to-open transition occurs at ~4.2 ns and is shown with a vertical line. In (B), the dihedral angles are shown in blue (ψ, Gly110), black (φ, Ser111), purple (ψ, Pro112), and green (φ, Thr113). In (C), the presence of a given hydrogen bond at any time point in the trajectory is indicated with a vertical line. Italics indicate that side chain atoms are involved in the hydrogen bonds. The sidechain of Gln128 is involved in two of the three hydrogen bonds.

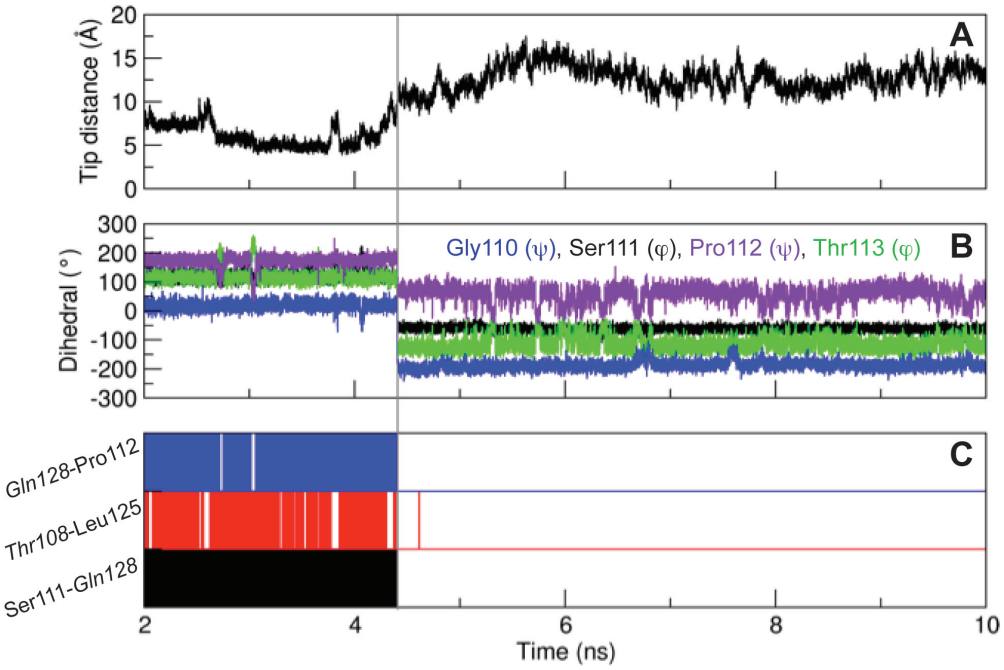

Table S1. Probabilities of hydrogen bonds that are correlated with the closed loop conformation. For Y123W C1Bα, the probabilities were calculated for the first part of the trajectory (between 2 and 10 ns) where the opening of the binding loops occurs.

Donor	Acceptor	*Y123W C1Bα*				*Wild-type C1Bα*
		T1[a]	T2	T3	mean[b]	mean[b]
Primary hydrogen bonds						
Thr108[c]	Leu125	–	0.17	0.75	–	Not present
Ser111	*Gln128*	–	0.30	0.76	–	
Gln128	Pro112	–	0.27	0.72	–	
Secondary hydrogen bonds						
Gln128	Leu122	0.23	0.61	0.99	0.61 ± 0.38	0.36 ± 0.44
Gly129	His107	0.24	0.61	0.99	0.61 ± 0.38	0.13 ± 0.06
Tyr109	*Gln128*	0.47	0.88	1.00	0.78 ± 0.28	0.51 ± 0.49

[a] T1, T2, and T3 are the individual trajectories for Y123W C1Bα.
[b] The mean probability and error were calculated using data from three trajectories.
[c] Italics indicate sidechain atoms.

Figure S7. Sidechain dihedral angles of Gln128 in wt and Y123W C1Bα. The angles are shown as a function of time for three trajectories (black, green, and red). The range sampled by χ_1, χ_2, and χ_3 indicates high mobility of Gln128 sidechain in both wt and mutant. The χ_3 dihedral angle defined by Cβ-Cγ-Cδ-Nε atoms often rotates 360° in the wt C1Bα. The sidechain rotations appear to occur less frequently in the mutant than in the wt.